



Available online at www.sciencedirect.com



International Journal of Solids and Structures 43 (2006) 4777–4794

INTERNATIONAL JOURNAL OF
SOLIDS and
STRUCTURES

www.elsevier.com/locate/ijsolstr

Cracked infinite cylinder with two rigid inclusions under axisymmetric tension

M. Evren Toygar ^{a,*}, M. Ruşen Geçit ^b

^a Dokuz Eylül University, Department of Mechanical Engineering, 35100 Izmir, Turkey

^b Middle East Technical University, Department of Engineering Sciences, 06531 Ankara, Turkey

Received 1 April 2005

Available online 8 September 2005

Abstract

This paper considers the problem of an axisymmetric infinite cylinder with a ring shaped crack at $z = 0$ and two ring-shaped rigid inclusions with negligible thickness at $z = \pm L$. The cylinder is under the action of uniformly distributed axial tension applied at infinity and its lateral surface is free of traction. It is assumed that the material of the cylinder is linearly elastic and isotropic. Crack surfaces are free and the constant displacements are continuous along the rigid inclusions while the stresses have jumps. Formulation of the mixed boundary value problem under consideration is reduced to three singular integral equations in terms of the derivative of the crack surface displacement and the stress jumps on the rigid inclusions. These equations, together with the single-valuedness condition for the displacements around the crack and the equilibrium equations along the inclusions, are converted to a system of linear algebraic equations, which is solved numerically. Stress intensity factors are calculated and presented in graphical form.

© 2005 Elsevier Ltd. All rights reserved.

Keywords: Fracture mechanics; Crack; Stress intensity factor; Inclusion; Singular integral equation

1. Introduction

Many unexpected failures of equipments and various machines have occurred throughout the industrial world. It is seen that many failures have been caused by preexisting notches or flaws in the materials that initiate cracks. These initial cracks propagate under service loading and finally may lead to a complete failure of the structure. Crack growth occurs generally through opening of a gap between the crack surfaces.

* Corresponding author.

E-mail address: evren.toygar@deu.edu.tr (M.E. Toygar).

Stresses near the crack tips become infinitely large and therefore the stress state at the crack tips can conveniently be defined by the stress intensity factors (SIFs).

In the early studies, for example, the effect of a penny-shaped crack on the distribution of stresses in an infinitely long cylinder has been studied in Sneddon and Tait (1963). A pair of Gauss–Chebyshev integration formulas for singular integrals has been developed in Erdogan and Gupta (1972). Using these formulas a simple numerical method for solving a system of singular integral equations has been described. The axisymmetric semi-infinite cylinder with fixed short end has been analyzed in Gupta (1974). Normal loads have been prescribed far away from the fixed end. An integral transform technique to formulate the problem in terms of a singular integral equation has been used. Stresses along the rigid end and stress intensity factors have been computed numerically. A semi-infinite elastic strip containing a transverse central crack has been considered in Turgut and Geçit (1988). Formulation has been reduced to a system of three singular integral equations. The elastostatic plane problem of a finite strip has been solved by Geçit and Turgut (1988) in which the solution of the problem has been obtained by considering (i) an infinite strip containing a transverse rigid inclusion at the middle and (ii) two symmetrically located transverse cracks. The general plane problem for an infinite strip containing multiple cracks perpendicular to its boundaries has been considered in Civelek and Erdogan (1982) by using the method of singular integral equations. The problem of a hollow cylinder containing an arbitrarily oriented radial crack has been analyzed in Delale and Erdogan (1982). The cylinder has been subjected to arbitrary normal tractions on the crack surfaces. Problem has been formulated in terms of a singular integral equation by using the basic dislocation solutions as the green's functions. The elasticity problem for a long hollow circular cylinder containing an axisymmetric circumferential crack has been considered in Nied and Erdogan (1983). The problem has been formulated in terms of a system of singular integral equations with the Fourier coefficients of the derivative of the crack surface displacement density functions. The SIFs and the crack opening displacement have been calculated. Again the SIFs and stress distributions in solid or hollow cylindrical bars with axisymmetric internal or edge crack have been investigated by Erdol and Erdogan (1978) using the standard transform technique.

In the present study, the SIFs for an infinitely long elastic solid cylinder containing a ring shaped crack whose surfaces are free of tractions and two ring-shaped rigid inclusions symmetrically located on both sides of the crack with arbitrary but equal widths are calculated. The solid cylinder is under the action of axisymmetric tensile loads at infinity. Material of the cylinder is assumed to be linearly elastic and isotropic. The main objective of this study is to have a good acquaintance with the mathematical difficulties in such a problem for a solid cylinder containing cracks and rigid inclusions, and also to have a good idea on the interaction of cracks and inclusions for this particular geometry and to calculate SIFs at the edges of the flaws.

2. Formulation and integral equations

Consider the axisymmetric problem for the solid cylindrical bar shown in Fig. 1. The infinite solid cylinder contains a ring-shaped crack of width $(b - a)$ at the symmetry plane $z = 0$ and two ring shaped rigid inclusions of width $(d - c)$ at $z = \pm L$ planes. The surfaces of the crack are free of tractions. The displacements are constant and continuous whereas stresses have jumps along the rigid inclusions with negligible thickness. The cylinder with radius A is subjected to uniformly distributed axial tension of intensity p_0 at infinity. Therefore, the governing equations of the axisymmetric elasticity problems must be solved under the following boundary conditions:

$$\sigma_z(r, 0) = 0, \quad a < r < b, \quad (1a)$$

$$w(r, 0) = 0, \quad 0 < r < a, \quad b < r < A, \quad (1b)$$

$$\sigma_z(r, +\infty) = p_0, \quad 0 < r < A, \quad (2a)$$

$$\sigma_z(r, -\infty) = p_0, \quad 0 < r < A, \quad (2b)$$

$$u(r, +L) = 0, \quad c < r < d, \quad (3a)$$

$$u(r, -L) = 0, \quad c < r < d, \quad (3b)$$

$$w(r, +L) = \text{const.}, \quad c < r < d, \quad (3c)$$

$$w(r, -L) = \text{const.}, \quad c < r < d, \quad (3d)$$

$$\sigma_r(A, z) = 0, \quad -\infty < z < \infty, \quad (4a)$$

$$\tau_{rz}(A, z) = 0, \quad -\infty < z < \infty, \quad (4b)$$

where u and w are the r - and z -components of the displacement vector, σ and τ denote the normal and shearing stresses, respectively. Solution for the problem shown in Fig. 1 may be obtained conveniently by superposing the solutions for (1) an infinite cylinder subjected to uniformly distributed tensile axial loads at infinity, and (2) an infinite cylinder having a ring-shaped crack at $z = 0$ and two rigid inclusions at $z = \pm L$ (perturbation problem). The external load in the perturbation problem is the negative of the stresses at location of the crack and the displacements at locations of the inclusions obtained from the first problem. Solution for the displacement and the stress components for the first problem is obtained easily in the form (Toygar, 1998)

$$u(r) = -\frac{(\kappa - 3)p_0}{2\mu(\kappa - 7)}r, \quad (5a)$$

$$w(z) = \frac{-2p_0}{\mu(\kappa - 7)}z, \quad (5b)$$

$$\sigma_r(r, z) = 0, \quad (6a)$$

$$\sigma_z(r, z) = p_0, \quad (6b)$$

$$\tau_{rz}(r, z) = 0, \quad (6c)$$

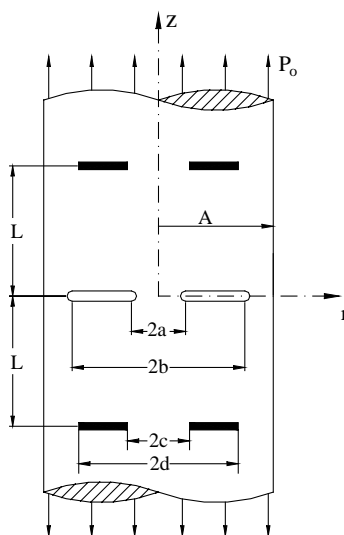


Fig. 1. Geometry and loading for the infinite cylinder with crack and inclusions.

where μ is the shear modulus, $\kappa = 3 - 4v$, v being the Poisson's ratio. Note here that the problem exhibits symmetry about $z = 0$ plane. Hence, only one half ($z \geq 0$) of it is considered.

General expressions for the stresses and the displacements for the perturbation problem must contain sufficient number of unknowns so that all of the boundary conditions (1)–(4) can be satisfied. Therefore, the following three sub-problems shown in Fig. 2 are considered.

(I) An infinite axisymmetric elastic medium with no crack or inclusions: General expressions are obtained by using Fourier sine/cosine transforms on z in the form (Toygar, 1998)

$$u(r, z) = \frac{2}{\pi} \int_0^\infty \left[-\frac{1}{2} c_1 I_1(\rho r) + c_2 \rho r I_0(\rho r) \right] \cos(\rho z) d\rho, \quad (7a)$$

$$w(r, z) = \frac{2}{\pi} \int_0^\infty \left\{ \frac{1}{2} c_1 I_0(\rho r) - c_2 [(\kappa + 1) I_0(\rho r) + \rho r I_1(\rho r)] \right\} \sin(\rho z) d\rho, \quad (7b)$$

$$\sigma_r(r, z) = \frac{2\mu}{\pi} \int_0^\infty \left\{ c_1 \left[-I_0(\rho r) + \frac{1}{\rho r} I_1(\rho r) \right] + c_2 [(\kappa - 1) I_0(\rho r) + 2\rho r I_1(\rho r)] \right\} \rho \cos(\rho z) d\rho, \quad (8a)$$

$$\sigma_z(r, z) = \frac{2\mu}{\pi} \int_0^\infty \{c_1 I_0(\rho r) - c_2 [(\kappa + 5) I_0(\rho r) + 2\rho r I_1(\rho r)]\} \rho \cos(\rho z) d\rho, \quad (8b)$$

$$\tau_{rz}(r, z) = \frac{2\mu}{\pi} \int_0^\infty \{c_1 I_1(\rho r) - c_2 [2\rho r I_0(\rho r) + (\kappa + 1) I_1(\rho r)]\} \rho \sin(\rho z) d\rho, \quad (8c)$$

where I_0 , I_1 are the modified Bessel functions of the first kind of order zero and one, respectively, c_1 , c_2 are yet unknowns.

(II) An infinite axisymmetric elastic medium containing a ring-shaped crack of width $(b - a)$ at $z = 0$: Navier equations are solved by the use of Hankel transform on r (Toygar, 1998)

$$u(r, z) = \frac{1}{\kappa + 1} \int_0^\infty M(\rho) (\kappa - 1 - 2\rho z) e^{-\rho z} J_1(\rho r) d\rho, \quad (9a)$$

$$w(r, z) = \frac{1}{\kappa + 1} \int_0^\infty M(\rho) (-\kappa - 1 - 2\rho z) e^{-\rho z} J_0(\rho r) d\rho, \quad (9b)$$

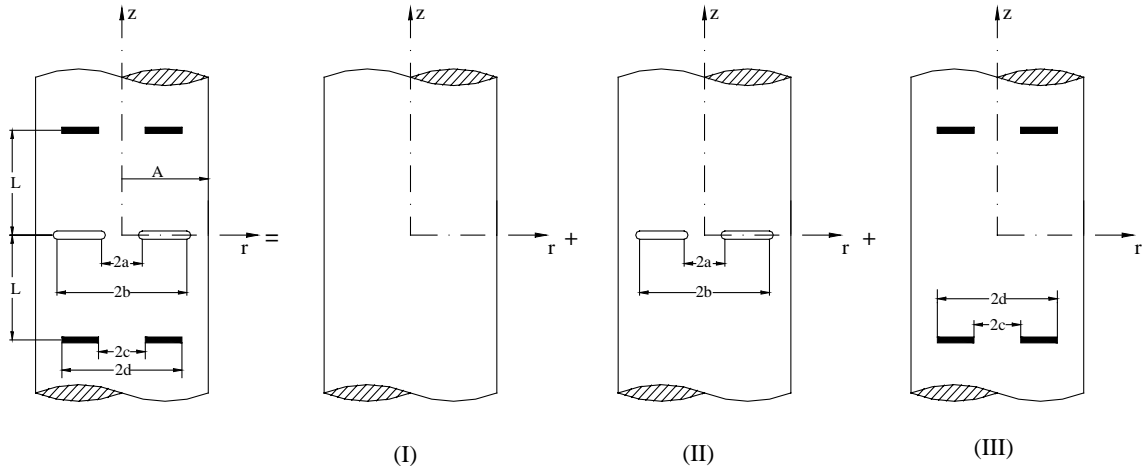


Fig. 2. Perturbation problem.

$$\sigma_r(r, z) = \frac{2\mu}{\kappa + 1} \int_0^\infty M(\rho) \left\{ [-2\rho z - (\kappa - 1)] \frac{1}{\rho r} J_1(\rho r) + 2(1 - \rho z) J_0(\rho r) \right\} \rho e^{-\rho z} d\rho, \quad (10a)$$

$$\sigma_z(r, z) = \frac{4\mu}{\kappa + 1} \int_0^\infty M(\rho) (1 + \rho z) \rho e^{-\rho z} J_0(\rho r) d\rho, \quad (10b)$$

$$\tau_{rz}(r, z) = \frac{4\mu}{\kappa + 1} \int_0^\infty M(\rho) \rho z \rho e^{-\rho z} J_1(\rho r) d\rho, \quad (10c)$$

where J_0 , J_1 are the Bessel functions of the first kind of order zero and one, respectively,

$$M(\rho) = \int_a^b m(r) r J_1(\rho r) dr, \quad (11)$$

$m(r)$ is the unknown crack surface displacement derivative

$$\frac{\partial}{\partial r} [w_1(r, 0) - w_2(r, 0)] = 2m(r), \quad a < r < b, \quad (12a)$$

$$m(r) = 0, \quad 0 < r < a, \quad b < r < A. \quad (12b)$$

(III) An infinite axisymmetric elastic medium containing two ring-shaped rigid inclusions of width $(d - c)$ at $z = \pm L$: Navier equations are solved again by the use of Hankel transform on r , and the following expressions may be written for the displacements and the stresses in $(-L \leq z \leq L)$ (Toygar, 1998)

$$\begin{aligned} u(r, z) = & \frac{1}{2\mu(\kappa + 1)} \int_0^\infty [(\rho(L - z) + \kappa) P_1(\rho) - \rho(L - z) P_2(\rho)] e^{\rho(L-z)} J_1(\rho r) d\rho \\ & + \frac{1}{2\mu(\kappa + 1)} \int_0^\infty [(-\rho(L + z) + \kappa) P_1(\rho) - \rho(L + z) P_2(\rho)] e^{-\rho(L+z)} J_1(\rho r) d\rho, \end{aligned} \quad (13a)$$

$$\begin{aligned} w(r, z) = & \frac{1}{2\mu(\kappa + 1)} \int_0^\infty [(-\rho(L - z) + \kappa) P_2(\rho) + \rho(L - z) P_1(\rho)] e^{\rho(L-z)} J_0(\rho r) d\rho \\ & + \frac{1}{2\mu(\kappa + 1)} \int_0^\infty [(-\rho(L + z) + \kappa) P_2(\rho) - \rho(L + z) P_1(\rho)] e^{-\rho(L+z)} J_0(\rho r) d\rho, \end{aligned} \quad (13b)$$

$$\begin{aligned} \sigma_r = & \frac{1}{2(\kappa + 1)} \int_0^\infty \left\{ [(-2\rho(L - z) - 2\kappa) P_1(\rho) + 2\rho(L - z) P_2(\rho)] e^{\rho(L-z)} \right. \\ & \left. + [(2\rho(L + z) - 2\kappa) P_1(\rho) + 2\rho(L + z) P_2(\rho)] e^{-\rho(L+z)} \right\} \frac{1}{r} J_1(\rho r) d\rho \\ & + \frac{1}{2(\kappa + 1)} \int_0^\infty \left\{ [(2\rho(L - z) + (\kappa + 3)) P_1(\rho) + (-2\rho(L - z) + (\kappa - 3)) P_2(\rho)] e^{\rho(L-z)} \right. \\ & \left. + [(-2\rho(L + z) + (\kappa + 3)) P_1(\rho) - (2\rho(L + z) + (\kappa - 3)) P_2(\rho)] e^{-\rho(L+z)} \right\} \rho J_0(\rho r) d\rho, \end{aligned} \quad (14a)$$

$$\begin{aligned} \sigma_z(r, z) = & \frac{1}{2(\kappa + 1)} \int_0^\infty \left\{ [(-2\rho(L - z) - (\kappa - 1)) P_1(\rho) + (2\rho(L - z) - (\kappa + 1)) P_2(\rho)] e^{\rho(L-z)} \right. \\ & \left. + [(2\rho(L + z) - (\kappa - 1)) P_1(\rho) + (2\rho(L + z) + (\kappa + 1)) P_2(\rho)] e^{-\rho(L+z)} \right\} \rho J_0(\rho r) d\rho, \end{aligned} \quad (14b)$$

$$\begin{aligned} \tau_{rz}(r, z) = & \frac{1}{2(\kappa + 1)} \int_0^\infty \left\{ [(-2\rho(L - z) - (\kappa + 1)) P_1(\rho) + (2\rho(L - z) - (\kappa - 1)) P_2(\rho)] e^{\rho(L-z)} \right. \\ & \left. + [(2\rho(L + z) - (\kappa + 1)) P_1(\rho) + (2\rho(L + z) + (\kappa - 1)) P_2(\rho)] e^{-\rho(L+z)} \right\} \rho J_1(\rho r) d\rho. \end{aligned} \quad (14c)$$

Here

$$P_1(\rho) = \int_c^d p_1(r) r J_1(\rho r) dr, \quad (15a)$$

$$P_2(\rho) = \int_c^d p_2(r) r J_0(\rho r) dr, \quad (15b)$$

where the unknown functions $p_1(r)$, $p_2(r)$ are the shearing and the normal stress jumps on the rigid inclusions,

$$\tau_{rz}(r, L^+) - \tau_{rz}(r, L^-) = p_1(r), \quad c < r < d, \quad (16a)$$

$$\sigma_{z_2}(r, L^+) - \sigma_{z_1}(r, L^-) = p_2(r), \quad c < r < d, \quad (16b)$$

satisfying the conditions

$$p_1(r) = p_2(r) = 0, \quad 0 \leq r < c, \quad d < r < A. \quad (17a, b)$$

When the general expressions for these three sub-problems are added together and substituted in the stress boundary conditions at the lateral surface of the solid cylinder, (4a) and (4b), the unknowns c_1 , c_2 are calculated. The general expressions for the perturbation problem are obtained in terms of the three unknown functions $M(\rho)$, $P_1(\rho)$, $P_2(\rho)$ which will be determined by using the boundary condition (1a) on the crack, (3a) and (3c) on the inclusions. It is noted that (3a) and (3c) are displacement type conditions whereas (1a) is a stress type condition. These three boundary conditions can be put into the form

$$\sigma_z(r, 0) = -p_0, \quad a < r < b, \quad (18)$$

$$\frac{\partial}{\partial r} w(r, L) = 0, \quad c < r < d, \quad (19a)$$

$$\frac{1}{r} \frac{\partial}{\partial r} [r u(r, L)] = \frac{3 - \kappa}{7 - \kappa} \frac{p_0}{\mu}, \quad c < r < d \quad (19b)$$

for the perturbation problem. Substituting the sum of the expressions given in (8b), (10b) and (14b) for the stress σ_z in (18); (7b), (9b) and (13b) for the displacement w in (19); and (7a), (9a) and (13a) for the displacement u in (19b), separating the divergent integrals giving the simple Cauchy-type singularity, Muskhelishvili (1953), after lengthy manipulations, the following singular integral equations are obtained (see Toygar (1998) for details):

$$\begin{aligned} & \frac{2\mu}{\pi} \int_a^b \left[\frac{2}{t-r} + 2H_1(r, t) + tN_{11}(r, t) \right] m(t) dt + \int_c^d t \left[T_1(r, t) - \frac{2}{\pi} N_{12}(r, t) \right] p_1(t) dt \\ & + \int_c^d t \left[T_2(r, t) - \frac{2}{\pi} N_{13}(r, t) \right] p_2(t) dt = -(\kappa + 1)p_0, \quad a < r < b, \end{aligned} \quad (20a)$$

$$\begin{aligned} & 2\mu \int_a^b t \left[T_3(r, t) + \frac{2}{\pi} N_{21}(r, t) \right] m(t) dt + \int_c^d t \left[T_4(r, t) - \frac{4}{\pi} N_{23}(r, t) \right] p_1(t) dt \\ & + \int_c^d \left[tT_5(r, t) + \frac{\kappa}{\pi} H_2(r, t) + \frac{\kappa}{\pi} \frac{1}{(t-r)} - \frac{4}{\pi} tN_{22}(r, t) \right] p_2(t) dt = 0, \quad c < r < d, \end{aligned} \quad (20b)$$

$$\begin{aligned} & 2\mu \int_a^b t \left[T_6(r, t) + \frac{2}{\pi} N_{31}(r, t) \right] m(t) dt + \int_c^d \left[tT_7(r, t) + \frac{\kappa}{\pi} H_3(r, t) + \frac{\kappa}{\pi} \frac{1}{t-r} - \frac{4}{\pi} tN_{33}(r, t) \right] p_1(t) dt \\ & - \int_c^d t \left[T_8(r, t) + \frac{4}{\pi} N_{32}(r, t) \right] p_2(t) dt = -2(\kappa + 1) \frac{3 - \kappa}{7 - \kappa} p_0, \quad c < r < d, \end{aligned} \quad (20c)$$

where

$$H_i(r, t) = \frac{m_i(r, t) - 1}{t - r}, \quad i = 1, \dots, 3, \quad (21a-c)$$

$$m_1(r, t) = \begin{cases} \frac{2(t-r)}{r} K\left(\frac{t}{r}\right) + \frac{2r}{t+r} E\left(\frac{t}{r}\right), & r > t \\ \frac{2t}{t+r} E\left(\frac{r}{t}\right), & r < t \end{cases}, \quad (22a)$$

$$m_2(r, t) = \begin{cases} \frac{2t}{t+r} E\left(\frac{t}{r}\right), & t < r \\ -\frac{2(t-r)}{r} K\left(\frac{r}{t}\right) + \frac{2r}{t+r} E\left(\frac{r}{t}\right), & t > r \end{cases}, \quad (22b)$$

$$m_3(r, t) = \begin{cases} \frac{2(t-r)}{r} K\left(\frac{t}{r}\right) + \frac{2r}{t+r} E\left(\frac{t}{r}\right), & r > t \\ \frac{2t}{t+r} E\left(\frac{r}{t}\right), & r < t \end{cases}, \quad (22c)$$

K and E are the complete elliptic integrals of the first and the second kinds, respectively. $N_{ij}(r, t)$ ($i, j = 1, \dots, 3$) are the kernels and $T_i(r, t)$ ($i = 1, \dots, 3$) are the elliptic integrals and are defined in the [Appendix A](#). Eq. (20a)–(20c), must be solved together with the following single-valuedness condition for the displacement around the crack

$$\int_a^b m(t) t dt = 0 \quad (23)$$

and the equilibrium conditions for the stresses on the rigid inclusions,

$$\int_c^d p_i(t) t dt = 0 \quad (i = 1, 2). \quad (24a, b)$$

When the integral equations (20a)–(20c) are examined closely, one may realize that

- (i) there are Cauchy-type singularities at $t = r$,
- (ii) the kernels H_{11} , H_{22} , H_{33} , have only logarithmic singularity at $\lambda = 0$,
- (iii) among the kernels N_{ij} , ($i, j = 1, \dots, 3$) only N_{11} , N_{22} , N_{33} have singular terms when $t = A$ and $r = A$. N_{ij} are all bounded when $r < A$ and can be written in the form

$$N_{ij}(r, t) = \int_0^\infty L_{ij}(r, t, \lambda) d\lambda, \quad (i, j = 1, \dots, 3). \quad (25)$$

Lengthy expressions for the integrands L_{ij} , ($i, j = 1, \dots, 3$) contain Bessel functions and are given in [Toygar \(1998\)](#). The singularity at zero may easily be removed by examining the behavior of integrands L_{ij} for $\lambda \rightarrow 0$ and giving regard to (23) and (24). It can be shown that the integrands of the kernels are bounded everywhere except for $\lambda = \infty$. By examining the asymptotic behavior of the integrands in (25) for $\lambda \rightarrow \infty$, the singular terms may be separated. Introduce the following notation:

$$N_{ijs}(r, t) = \int_0^\infty L_{ij\infty}(r, t, \lambda) d\lambda \quad (i, j = 1, \dots, 3), \quad (26a)$$

$$L_{ij\infty}(r, t, \lambda) = \lim_{\lambda \rightarrow \infty} L_{ij}(r, t, \lambda) \quad (i, j = 1, \dots, 3), \quad (26b)$$

in which the expressions for $L_{ij\infty}(r, t, \lambda)$, $(i, j = 1, \dots, 3)$ are given in the [Appendix A](#). The bounded parts of the kernels can then be expressed as

$$N_{ijb}(r, t) = N_{ij}(r, t) - N_{ijs}(r, t) \quad (i, j = 1, \dots, 3), \quad (27a)$$

$$N_{ijb}(r, t) = \int_0^\infty [L_{ij}(r, t, \lambda) - L_{ij\infty}(r, t, \lambda)] d\lambda \quad (i, j = 1, \dots, 3). \quad (27b)$$

By using the asymptotic expressions of modified Bessel functions, for positive values of r and t , the expressions for $L_{ij\infty}(r, t, \lambda)$ can be obtained and their integrals give

$$N_{11s}(r, t) = \left[-2 + 12(A - r) \frac{d}{dr} - 4(A - r)^2 \frac{d^2}{dr^2} \right] \left[\frac{1}{r + t - 2A} \right], \quad (28a)$$

$$N_{22s}(r, t) = \left[\frac{1}{4}(\kappa^2 - 3) + 3(A - r) \frac{d}{dr} - (A - r)^2 \frac{d^2}{dr^2} \right] \left[\frac{1}{r + t - 2A} \right], \quad (28b)$$

$$N_{33s}(r, t) = \left[\frac{1}{4}(\kappa^2 - 3) + 3(A - r) \frac{d}{dr} - (A - r)^2 \frac{d^2}{dr^2} \right] \left[\frac{1}{r + t - 2A} \right]. \quad (28c)$$

Together with the simple Cauchy kernel, $1/(t - r)$, N_{11} , N_{22} , N_{33} constitute generalized Cauchy kernels. The unknown functions $m(t)$, $p_1(t)$ and $p_2(t)$ have integrable singularities at the end points. Writing

$$m(t) = M^*(t)[(t - a)(b - t)]^{-\gamma}, \quad 0 < \operatorname{Re}(\gamma) < 1, \quad (29a)$$

$$p_i(t) = P_i^*(t)[(t - c)(d - t)]^{-\delta} \quad (i = 1, 2), \quad 0 < \operatorname{Re}(\delta) < 1, \quad (29b, c)$$

where $M^*(t)$, $P_i^*(t)$ ($i = 1, 2$) are Hölder-continuous functions in the respective intervals $[a, b]$ and $[c, d]$, after somewhat routine manipulations, [Toygar \(1998\)](#), it can be shown that γ and δ satisfy the characteristic equations

$$\cot \pi \gamma = 0, \quad (30a)$$

$$\cot \pi \delta = 0, \quad (30b)$$

which give $\gamma = 1/2$ at the edges of the crack ($r \rightarrow a$, $r \rightarrow b$) and $\delta = 1/2$ at the edges of the inclusions ($r \rightarrow c$, $r \rightarrow d$). The system of three singular integral equations [\(20a\)–\(20c\)](#), with the single-valuedness condition [\(23\)](#) and the equilibrium conditions [\(24a,b\)](#), are first normalized and then by using the Gauss–Lobatto integration formula, are put into the form of a system of linear algebraic equations. Introducing the dimensionless variables α , ξ on the crack and η , β on the inclusions by the relations

$$t = \frac{b - a}{2} \alpha + \frac{b + a}{2}, \quad a < t < b, \quad -1 < \alpha < 1, \quad (31a)$$

$$r = \frac{b - a}{2} \xi + \frac{b + a}{2}, \quad a < r < b, \quad -1 < \xi < 1, \quad (31b)$$

$$t = \frac{d - c}{2} \eta + \frac{d + c}{2}, \quad c < t < d, \quad -1 < \eta < 1, \quad (31c)$$

$$r = \frac{d - c}{2} \beta + \frac{d + c}{2}, \quad c < r < d, \quad -1 < \beta < 1, \quad (31d)$$

the integral equations (20a)–(20c), (23) and (24a,b) may be written in the form

$$\begin{aligned} \frac{2\mu}{\pi} \int_{-1}^1 \bar{m}(\alpha) \left[\bar{H}_1(\xi, \alpha) + \frac{2}{\alpha - \xi} + \hat{N}_{11}(\xi, \alpha) \right] d\alpha + \frac{1}{\pi} \int_{-1}^1 \bar{p}_1(\eta) [\bar{T}_1(\xi, \eta) - \bar{N}_{12}(\xi, \eta)] d\eta \\ + \frac{1}{\pi} \int_{-1}^1 \bar{p}_2(\eta) [\bar{T}_2(\xi, \eta) - \bar{N}_{13}(\xi, \eta)] d\eta = -(\kappa + 1)p_0, \quad -1 < \xi < 1, \end{aligned} \quad (32a)$$

$$\begin{aligned} \frac{2\mu}{\pi} \int_{-1}^1 \bar{m}(\alpha) \left[\hat{T}_3(\beta, \alpha) + \hat{N}_{21}(\beta, \alpha) \right] d\alpha + \frac{1}{\pi} \int_{-1}^1 \bar{p}_1(\eta) [\bar{T}_4(\beta, \eta) - \bar{N}_{23}(\beta, \eta)] d\eta \\ + \frac{1}{\pi} \int_{-1}^1 \bar{p}_2(\eta) \left[\bar{T}_5(\beta, \eta) - \bar{H}_2(\beta, \eta) + \frac{\kappa}{\eta - \beta} - \bar{N}_{22}(\beta, \eta) \right] d\eta = 0, \quad -1 < \beta < 1, \end{aligned} \quad (32b)$$

$$\begin{aligned} \frac{2\mu}{\pi} \int_{-1}^1 \bar{m}(\alpha) [\hat{T}_6(\beta, \alpha) + \hat{N}_{31}(\beta, \alpha)] d\alpha + \frac{1}{\pi} \int_{-1}^1 \bar{p}_1(\eta) \left[\bar{T}_7(\beta, \eta) + \bar{H}_3(\beta, \eta) + \frac{\kappa}{\eta - \beta} - \bar{N}_{33}(\beta, \eta) \right] d\eta \\ + \frac{1}{\pi} \int_{-1}^1 \bar{p}_2(\eta) [\bar{T}_8(\beta, \eta) - \bar{N}_{32}(\beta, \eta)] d\eta = -2(\kappa + 1) \frac{3 - \kappa}{7 - \kappa} p_0, \quad -1 < \beta < 1, \end{aligned} \quad (32c)$$

where

$$\bar{m}(\alpha) = m \left(\frac{b - a}{2} \alpha + \frac{b + a}{2} \right), \quad (33a)$$

$$\bar{p}_i(\eta) = p_i \left(\frac{d - c}{2} \eta + \frac{d + c}{2} \right) \quad (i = 1, 2). \quad (33b, c)$$

By substituting singular behavior of the dimensionless unknown functions

$$\bar{m}(\alpha) = \bar{M}(\alpha)(1 - \alpha^2)^{-1/2}, \quad -1 < \alpha < 1, \quad (34a)$$

$$\bar{p}_i(\eta) = \bar{P}_i(\eta)(1 - \eta^2)^{-1/2} \quad (i = 1, 2), \quad -1 < \eta < 1 \quad (34b, c)$$

and by using the Gauss–Lobatto integration formula, Stroud and Secrest (1966), (32a)–(32c) may be converted to a system of linear algebraic equations. This system is solved numerically. The infinite integrals are calculated using Laguerre and Filon integration formulas, Stroud and Secrest (1966). After the numerical solution is completed, mode I SIFs k_{1a}, k_{1b} at the edges of the crack, mode I SIFs k_{1c}, k_{1d} and mode II SIFs k_{2c}, k_{2d} at the edges of the rigid inclusions may be calculated

$$k_{1a} = \lim_{r \rightarrow a} \sqrt{2(a - r)} \sigma_z(r, 0), \quad (35a)$$

$$k_{1b} = \lim_{r \rightarrow b} \sqrt{2(r - b)} \sigma_z(r, 0), \quad (35b)$$

$$k_{1c} = \lim_{r \rightarrow c} \sqrt{2(c - r)} \sigma_z(r, L), \quad (36a)$$

$$k_{1d} = \lim_{r \rightarrow d} \sqrt{2(r - d)} \sigma_z(r, L), \quad (36b)$$

$$k_{2c} = \lim_{r \rightarrow c} \sqrt{2(c - r)} \tau_{rz}(r, L), \quad (36c)$$

$$k_{2d} = \lim_{r \rightarrow d} \sqrt{2(r - d)} \tau_{rz}(r, L). \quad (36d)$$

3. Numerical results and discussion

Some of the calculated results are presented in graphical form in Figs. 3–12 for the normalized SIFs at the edges of the crack

$$k_{\overline{1a}} = k_{1a}/p_0 \sqrt{(b-a)/2}, \quad (37a)$$

$$k_{\overline{1b}} = k_{1b}/p_0 \sqrt{(b-a)/2} \quad (37b)$$

and the normalized SIFs at the edges of the inclusions

$$k_{\overline{1c}} = k_{1c}/p_0 \sqrt{(d-c)/2}, \quad (38a)$$

$$k_{\overline{1d}} = k_{1d}/p_0 \sqrt{(d-c)/2}, \quad (38b)$$

$$k_{\overline{2c}} = k_{2c}/p_0 \sqrt{(d-c)/2}, \quad (38c)$$

$$k_{\overline{2d}} = k_{2d}/p_0 \sqrt{(d-c)/2}. \quad (38d)$$

Table 1 shows the comparison of the results for $k_{\overline{1a}}$, $k_{\overline{1b}}$ when $L/A \rightarrow \infty$ with Nied and Erdogan (1983) for a particular geometry. Table indicates a pretty good agreement.

Figs. 3–5 show the normalized SIFs $k_{\overline{1a}}$, $k_{\overline{1b}}$ at the edges of the crack whose centerline is at $r = A/2$ since $a + b = A$. Centerline of the inclusions is also at $r = A/2$ since $c + d = A$ too. Fig. 3 gives variations with the crack width when $L/A = 1$ and $v = 0.3$. It seems that both SIFs increase when the crack width increases. $k_{\overline{1a}}$ is more sensitive to crack width and is greater than $k_{\overline{1b}}$. Both are larger for wider inclusions. Fig. 4 gives variations of $k_{\overline{1a}}$ and $k_{\overline{1b}}$ with inclusion width when $L/A = 0.5$, $b - a = 0.8A$ and centerlines of the crack and the inclusions are all at $r = A/2$ again for various v values. $k_{\overline{1a}}$ seems to be sensitive to v for relatively wider inclusions while $k_{\overline{1b}}$ seems to be practically independent of v . $k_{\overline{1a}}$ is always larger than $k_{\overline{1b}}$. Fig. 5 shows variations of normalized SIFs $k_{\overline{1a}}$, $k_{\overline{1b}}$ at the edges of the crack with L/A when $a + b = A$, $c + d = A$,

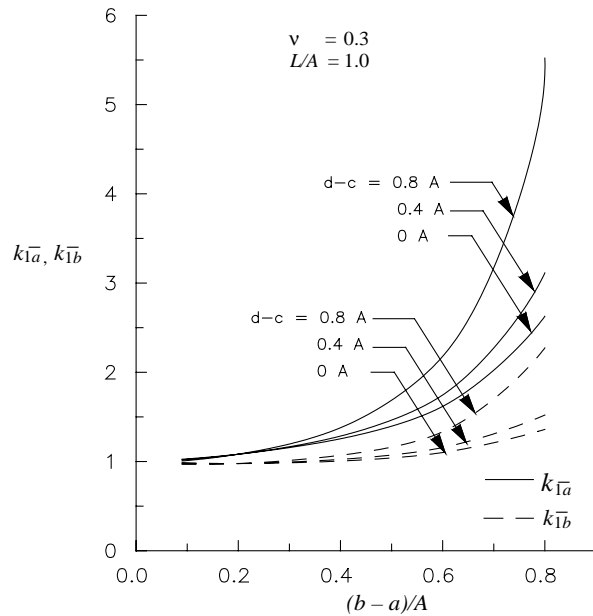


Fig. 3. Variation of the normalized stress intensity factors $k_{\overline{1a}}$, $k_{\overline{1b}}$ with $(b-a)/A$ when $L = A$, $a + b = A$, $c + d = A$, $v = 0.3$.

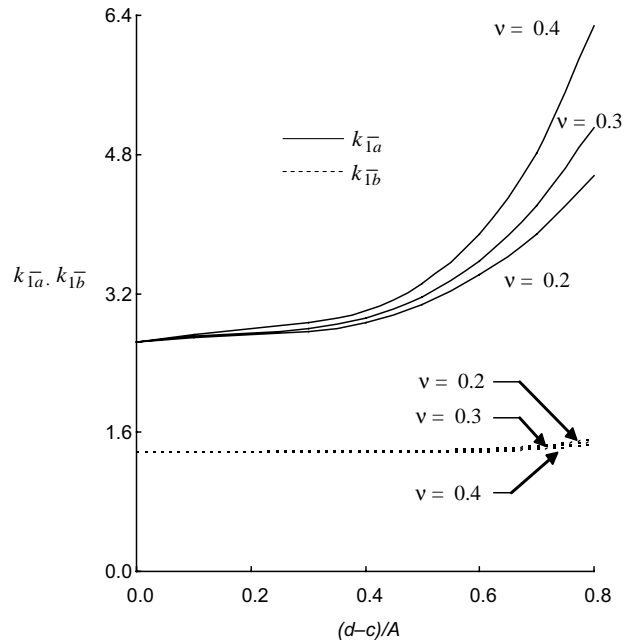


Fig. 4. Variation of the normalized stress intensity factors k_{1a} , k_{1b} with $(d - c)/A$ when $L = 0.5A$, $b - a = 0.8A$, $a + b = A$, $c + d = A$.

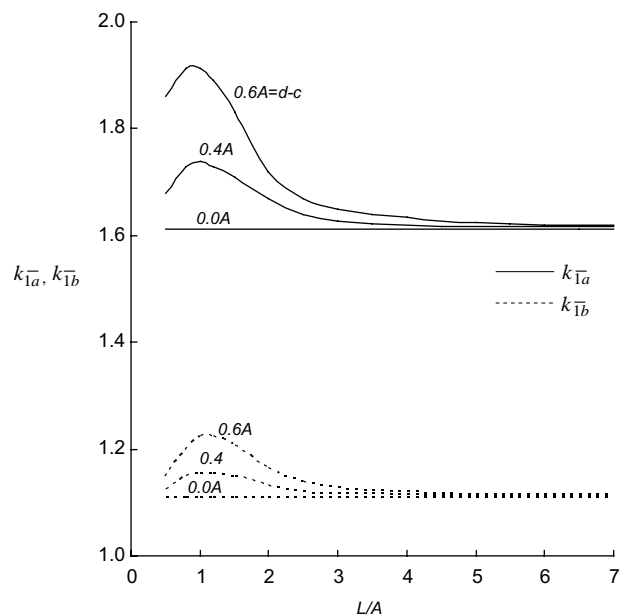


Fig. 5. Variation of the normalized stress intensity factors k_{1a} , k_{1b} with L/A when $a + b = A$, $c + d = A$, $b - a = 0.6A$, $v = 0.3$.

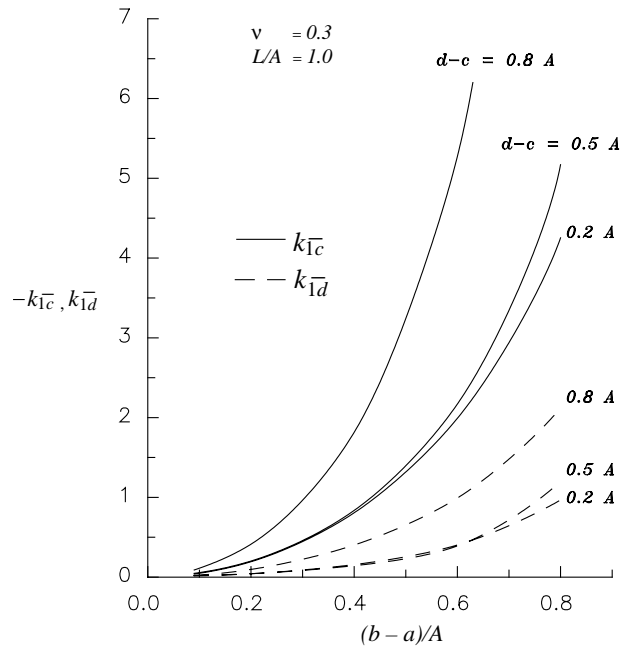


Fig. 6. Variation of the normalized stress intensity factors k_{1c}^- , k_{1d}^- with $(b-a)/A$ when $L = A$, $a + b = A$, $c + d = A$, $v = 0.3$.

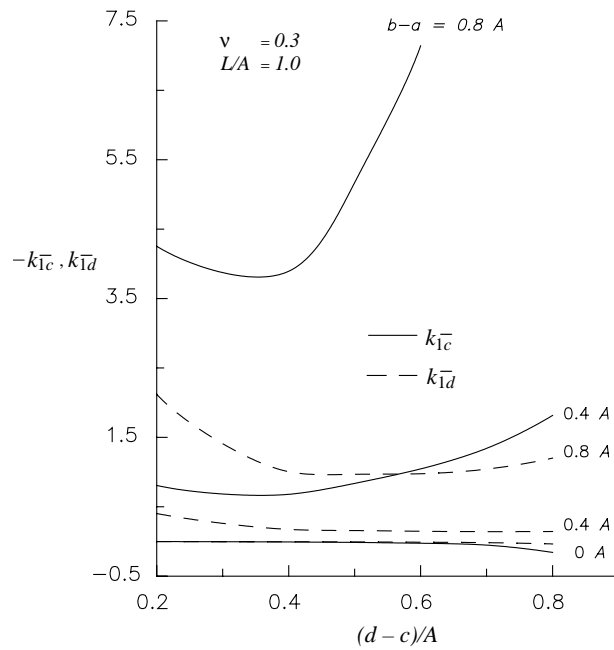


Fig. 7. Variation of the normalized stress intensity factors k_{1c}^- , k_{1d}^- with $(d-c)/A$ when $L = A$, $a + b = A$, $c + d = A$, $v = 0.3$.

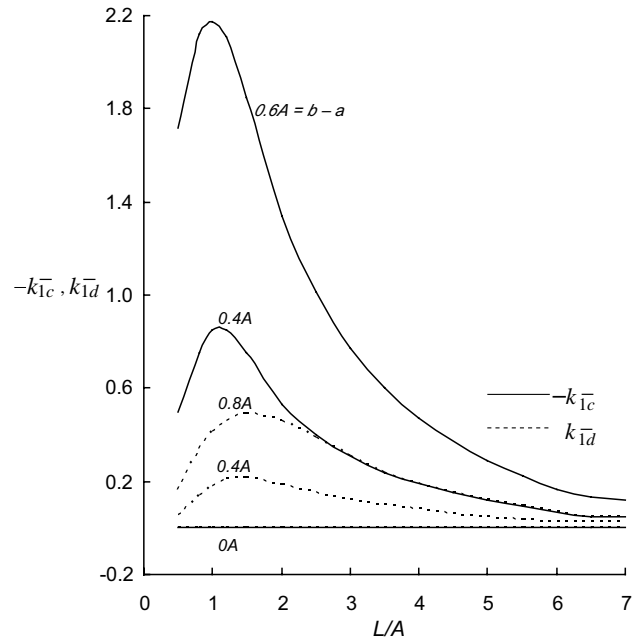


Fig. 8. Variation of the normalized stress intensity factors k_{1c}^- , k_{1d}^- with L/A when $a + b = A$, $c + d = A$, $d - c = 0.5A$, $v = 0.3$.

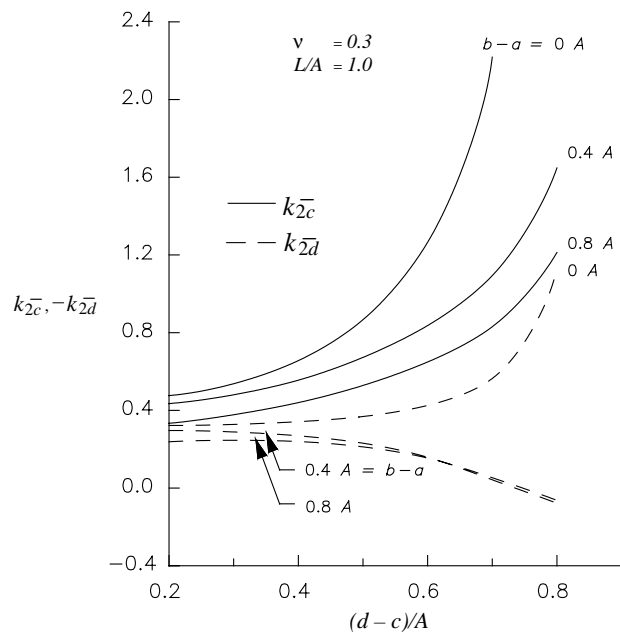


Fig. 9. Variation of the normalized stress intensity factors k_{2c}^- , k_{2d}^- with $(d - c)/A$ when $L = A$, $a + b = A$, $c + d = A$, $v = 0.3$.

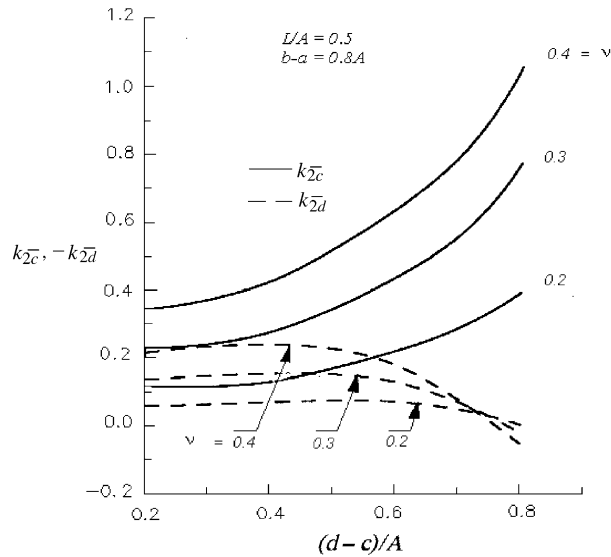


Fig. 10. Variation of the normalized stress intensity factors k_{2c} , k_{2d} with $(d-c)/A$ when $L = 0.5A$, $b - a = 0.8A$, $a + b = A$, $c + d = A$.

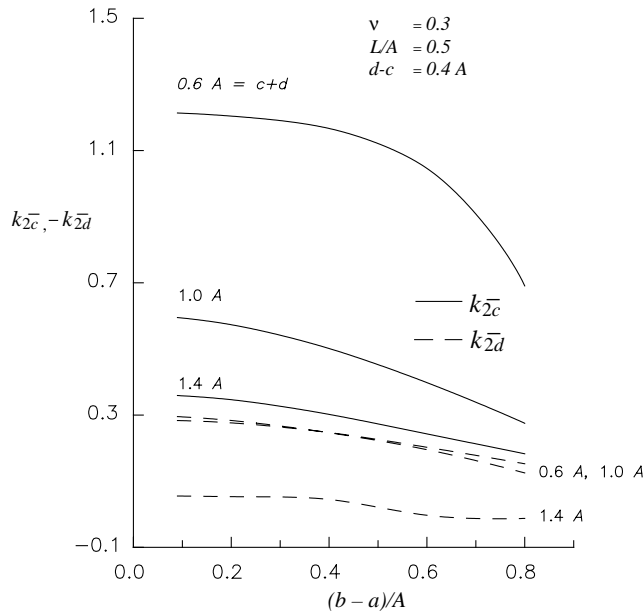


Fig. 11. Variation of the normalized stress intensity factors k_{2c} , k_{2d} with $(b-a)/A$ when $L = 0.5A$, $d - c = 0.4A$, $a + b = A$, $v = 0.3$.

$b - a = 0.6A$ and $v = 0.3$. Three inclusion widths are considered: 0, $0.4A$, $0.6A$. It seems that the effect of the inclusions on the crack is maximum when $L/A \approx 1$ and this effect vanishes practically when $L/A > 5$.

Figs. 6–8 show the normalized mode I SIFs k_{1c} , k_{1d} at the edges of the inclusions whose centerline as well as the centerline of the crack are at $r = A/2$. In Figs. 6 and 7, $L/A = 1$ and $v = 0.3$. As can be seen from

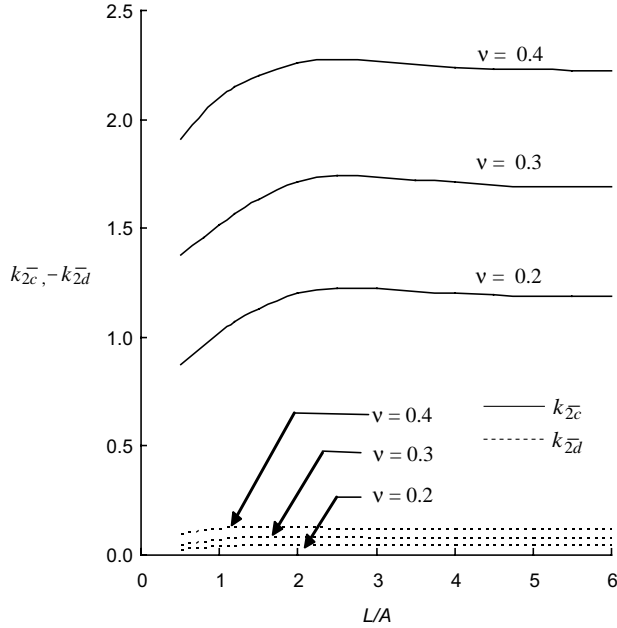


Fig. 12. Variation of the normalized stress intensity factors k_{2c}^- , k_{2d}^- with L/A when $a + b = A$, $c + d = A$, $b - a = 0.6A$, $d - c = 0.8A$.

Table 1
Comparison of k_{1a}^- , k_{1b}^- when $L/A \rightarrow \infty$ for $a = 0.505A$, $b = 0.595A$, $c + d = A$

	Nied and Erdogan	Present study
k_{1a}^-	1.028	1.024
k_{1b}^-	0.989	0.984

Fig. 6, k_{1c}^- and k_{1d}^- both increase monotonically as the crack width increases when $d - c = 0.2A$, $0.5A$, or $0.8A$. Fig. 7 shows that, for relatively wide cracks, e.g., when $b - a = 0.8A$, k_{1c}^- and k_{1d}^- first decrease as the inclusions get wider up to $d - c \approx 0.5A$ and then increase as $d - c$ increases further. This may be due to the fact that crack edges create more disturbed stress fields in comparison with inclusion edges. k_{1c}^- seems to be more sensitive and is always larger than k_{1d}^- . Fig. 8 shows variations of k_{1c}^- , k_{1d}^- at the edges of the inclusions with L/A when $a + b = A$, $c + d = A$, $d - c = 0.5A$ and $v = 0.3$. Three crack widths are considered: 0, $0.4A$, $0.6A$. Maximum interaction is observed when $L/A \approx 1$ and it fades away when $L/A > 7$.

Figs. 9–11 show variations of the normalized mode II SIFs k_{2c}^- and k_{2d}^- at the edges of the inclusions with crack and inclusion widths. In Fig. 9, $L/A = 1$, $v = 0.3$ and all centerlines are at $r = A/2$. k_{2c}^- increases considerably as $d - c$ increases and/or $b - a$ decreases. On the other hand, k_{2d}^- decreases as $d - c$ increases and seems to be slightly effected when $b - a$ changes for relatively large values of $d - c$. In Fig. 10, $L/A = 0.5$, $b - a = 0.8A$ and all centerlines are at $r = A/2$. k_{2c}^- increases as $d - c$ and/or v increases. In general, k_{2d}^- is larger for larger v , except for $d - c > 0.74A$. Note that the inclusions become ineffective as v decreases, i.e., as Poisson's effect diminishes. In Fig. 11, $L/A = 0.5$, $d - c = 0.4A$, $v = 0.3$ and the centerline of the crack is at $r = A/2$. As $c + d$ increases, the inclusions with constant width $0.4A$ move outward and k_{2c}^- decreases. k_{2c}^- and k_{2d}^- decrease when $b - a$ increases.

Fig. 12 shows variations of the normalized SIF's $k_{\overline{2c}}$ and $k_{\overline{2d}}$ at the edges of the inclusions with L/A when $a+b=A$, $c+d=A$, $b-a=0.6A$ and $d-c=0.8A$. Three values for ν are considered: 0.2, 0.3, 0.4. $k_{\overline{2c}}$ and $k_{\overline{2d}}$ both increase as L/A increases up to ≈ 2.5 , after slight decreases until ≈ 5 , remain constant afterwards.

4. Conclusions

The effect of two rigid inclusions on crack propagation in an axisymmetric infinite cylinder under uniaxial tension is being examined. The normalized SIFs for crack and inclusions are computed and presented in graphical form. It is observed that the normalized mode I SIFs at the edges of the crack and at the edges of the inclusions increase with increasing inclusion width while crack is propagating radially. However, the normalized mode II SIFs at the edges of the inclusions decrease with increase in inclusion width. As the crack gets closer to the circumference of the cylinder, considerable increase is observed in the normalized SIFs. As the inclusions get farther from the crack, the normalized mode I SIFs at the edges of the crack and the inclusions decrease, but the normalized mode II SIFs at the edges of the inclusions increase. Interaction fades away when $L/A > \approx 7$. It is also observed that the SIFs are influenced by the material property which is brought into consideration by the Poisson's ratio. As the Poisson's ratio becomes smaller, the effect of the rigid inclusions becomes smaller too.

Appendix A

Expressions of the infinite integrals appearing in Eq. (20a)–(20c) are

$$N_{ij} = \int_0^\infty L_{ij\infty}(r, t, \lambda) d\lambda + \int_0^\infty [L_{ij}(r, t, \lambda) - L_{ij\infty}(r, t, \lambda)] d\lambda, \quad i = 1, \dots, 3, \quad j = 1, \dots, 3, \quad (\text{A.1})$$

where the unbounded integrands are given in the form

$$\begin{aligned} L_{11\infty} &= \frac{e^{-\lambda(2A-r-t)}}{\sqrt{rt}} \{ -4(A-r)(A-t)\lambda^2 + 2(A-r)\lambda + 6(A-t)\lambda - 4 \}, \\ L_{12\infty} &= \frac{e^{-\lambda(2A-r-t)}}{\sqrt{rt}} \cos \lambda L \left\{ 2(A-r)(A-t)\lambda^2 + \kappa(A-r)\lambda - 3(A-t)\lambda - \frac{1}{2}(3\kappa-1) \right\}, \\ L_{13\infty} &= \frac{e^{-\lambda(2A-r-t)}}{\sqrt{rt}} \sin \lambda L \left\{ -2(A-r)(A-t)\lambda^2 + \kappa(A-r)\lambda + 3(A-t)\lambda - \frac{1}{2}(3\kappa+1) \right\}, \\ L_{21\infty} &= \frac{e^{-\lambda(2A-r-t)}}{\sqrt{rt}} \left\{ -2(A-r)(A-t)\lambda^2 + (A-r)(A-t)(\kappa+2)\lambda - \frac{1}{2}(\kappa+3) \right\}, \\ L_{22\infty} &= \frac{e^{-\lambda(2A-r-t)}}{\sqrt{rt}} \cos \lambda L \left\{ (A-r)(A-t)\lambda^2 + \frac{\kappa}{2}(A-r)\lambda - \left(\frac{\kappa}{2}+1\right)(A-t)\lambda - \frac{1}{4}(\kappa^2+2\kappa-1) \right\}, \\ L_{23\infty} &= \frac{e^{-\lambda(2A-r-t)}}{\sqrt{rt}} \sin \lambda L \left\{ -(A-r)(A-t)\lambda^2 + \frac{\kappa}{2}(A-r)\lambda + \left(\frac{\kappa}{2}+1\right)(A-t)\lambda - \frac{1}{4}(\kappa^2+2\kappa+1) \right\}, \\ L_{31\infty} &= \frac{e^{-\lambda(2A-r-t)}}{\sqrt{rt}} \left\{ 2(A-r)(A-t)\lambda^2 - (A-r)\lambda + (\kappa-2)(A-t)\lambda - \frac{1}{4}(\kappa-3) \right\}, \\ L_{32\infty} &= \frac{e^{-\lambda(2A-r-t)}}{\sqrt{rt}} \cos \lambda L \left\{ -(A-r)(A-t)\lambda^2 - \frac{\kappa}{2}(A-r)\lambda - \left(\frac{\kappa}{2}-1\right)(A-t)\lambda - \frac{1}{4}(\kappa-1) \right\}, \end{aligned}$$

$$L_{33\infty} = \frac{e^{-\lambda(2A-r-t)}}{\sqrt{rt}} \sin \lambda L \left\{ (A-r)(A-t)\lambda^2 - \frac{\kappa}{2}(A-r)\lambda + \frac{1}{2}(\kappa-2)(A-t)\lambda - \frac{1}{4}(\kappa^2 - 2\kappa - 1) \right\}, \quad (\text{A.2})$$

$T_i(r, t)$, ($i = 1, \dots, 8$), the elliptic integrals, are defined as follows:

$$\begin{aligned} T_1(r, t) &= 2Lg(r, t) - (\kappa - 1)h(r, t), \\ T_2(r, t) &= 2Lp(r, t) + (\kappa + 1)q(r, t), \\ T_3(r, t) &= 2La(r, t) + (\kappa + 1)b(r, t), \\ T_4(r, t) &= 2Lc(r, t), \\ T_5(r, t) &= 2Ld(r, t) - \kappa e(r, t), \\ T_6(r, t) &= -2Lg(r, t) + (\kappa - 1)h(r, t), \\ T_7(r, t) &= -2Lf(r, t) + \kappa n(r, t), \\ T_8(r, t) &= 2Lz(r, t), \end{aligned} \quad (\text{A.3})$$

in which

$$\begin{aligned} a(r, t) &= \int_0^\infty \rho^2 e^{-\rho L} J_1(\rho t) J_1(\rho r) d\rho, \\ b(r, t) &= \int_0^\infty \rho e^{-\rho L} J_1(\rho t) J_1(\rho r) d\rho, \\ c(r, t) &= \int_0^\infty \rho^2 e^{-\rho L} J_1(\rho t) J_0(\rho r) d\rho, \\ d(r, t) &= \int_0^\infty \rho^2 e^{-2\rho L} J_0(\rho t) J_1(\rho r) d\rho, \\ e(r, t) &= \int_0^\infty \rho e^{-2\rho L} J_0(\rho t) J_1(\rho r) d\rho, \\ f(r, t) &= \int_0^\infty \rho^2 e^{-2\rho L} J_1(\rho t) J_0(\rho r) d\rho, \\ g(r, t) &= \int_0^\infty \rho^2 e^{-\rho L} J_1(\rho t) J_0(\rho r) d\rho, \\ h(r, t) &= \int_0^\infty \rho e^{-\rho L} J_1(\rho t) J_0(\rho r) d\rho, \\ n(r, t) &= \int_0^\infty \rho e^{2\rho L} J_1(\rho t) J_0(\rho r) d\rho, \\ z(r, t) &= \int_0^\infty \rho^2 e^{-2\rho L} J_0(\rho t) J_0(\rho r) d\rho. \end{aligned} \quad (\text{A.4})$$

References

Civelek, M.B., Erdogan, F., 1982. Crack problems for a rectangular plate and an infinite strip. International Journal of Fracture 19, 139–159.

Delale, F., Erdogan, F., 1982. Stress Intensity factors in hollow cylinder containing a radial crack. International Journal of Fracture 20, 251–265.

Erdogan, F., Gupta, G.D., 1972. On the numerical solution of singular integral equations. Quarterly of Applied Mathematics 30, 525–534.

Erdol, R., Erdogan, F., 1978. A thick-walled cylinder with an axisymmetric internal or edge crack. *Journal of Applied Mechanics* 45, 281–296.

Geçit, M.R., Turgut, A., 1988. Extension of a finite strip bonded to a rigid support. *Computational Mechanics* 3, 398–410.

Gupta, G.D., 1974. The analysis of the semi-infinite cylinder problem. *International Journal of Solids and Structures* 10, 137–148.

Muskhelishvili, N.I., 1953. *Singular Integral Equations*. P. Noordhoff, Gröningen, Holland.

Nied, H.F., Erdogan, F., 1983. The elasticity problem for a thick-walled cylinder containing a circumferential crack. *International Journal of Fracture* 22, 277–301.

Sneddon, I.N., Tait, R.J., 1963. The effect of a penny-shaped crack on the distribution of stress in a long circular cylinder. *International Journal of Engineering Science* 1, 419–441.

Stroud, A.H., Secrest, D., 1966. *Gaussian Quadrature Formulas*. Prentice-Hall, New York.

Toygar, M.E., 1998. Infinite cylinder with a transverse crack and two rigid inclusions under axial tension. PhD Thesis, Middle East Technical University, Ankara, Turkey.

Turgut, A., Geçit, M.R., 1988. A semi-infinite elastic strip containing a transverse crack. *The Arabian Journal for Science and Engineering* 13, 71–80.